Journal of Coastal Research	SI	103	373–377	Coconut Creek, Florida	2020

Marine Current Generators Multimachine System Based on High Order Sliding Mode Control

Min Zhang*, Xihuai Wang, and Weijian Mi

Logistics Engineering College
Shanghai Marine University
Shanghai 201306, China

www.cerf-jcr.org

www.JCRonline.org

ABSTRACT

Zhang, M.; Wang, X., and Mi, W., 2020. Marine current generators multimachine system based on high order sliding mode control. *In*: Yang, Y.; Mi, C.; Zhao, L., and Lam, S. (eds.), *Global Topics and New Trends in Coastal Research: Port, Coastal and Ocean Engineering*. *Journal of Coastal Research*, Special Issue No. 103, pp. 373–377. Coconut Creek (Florida), ISSN 0749-0208.

Combined with high order sliding mode control, a nonlinear decentralized sliding mode strategy is proposed, which takes the marine current power station transient stability into consideration and introduces the high-order sliding mode to generators control rules. Achieving multimachine connect in independent power system by controlling each generator frequency and voltage. In addition, simulation results are presented robustness under mechanical perturbations.

ADDITIONAL INDEX WORDS: *Tidal generation, multimachine system, high order sliding mode, nonlinear.*

INTRODUCTION

Under the threat from global warming, tidal generation has received high attention due to its predictable, clean and abundant natures. Globally, the tidal energy is approximately 75 GW (Boye, Caquot, and Clement, 2013). In relation to China, the potential tidal energy can be up to 832.51 GW, and the capacity that can be technically developed is 166.49 GW, which is equivalent to 14586 GW•h each year (Bai *et al.*, 2016). This can alleviate the energy shortage of China.

Tidal energy is referred to as the energy generated by tidal movement. Tidal generation technology transfers tidal energy into mechanical energy using hydroturbine. In turn, the resulting mechanical energy will be transferred into electric energy through generators (Jiang *et al.*, 2019; Ma *et al.*, 2015; Ma *et al.*, 2018; Sun *et al.*, 2018; Xu *et al.*, 2015). Although tidal generation has a bright prospect, investigations of the control of tidal generators are rare. Fuzzy control and sliding mode control were applied to control the rotating speed of the permanent magnet synchronous generator by adjusting its reference current (Gu, Yin, and Liu, 2015). A PI controller was used to control the waveform of PWM, which, in turn, can control the output voltage and realize the connection between the system and power grid (Psillakis and Alexandridis, 2005).

Also, the investigations of multimachine system in the area of tidal generations are rarely implemented. In the structure of multimachine, WRSG can be directly applied for the connection of multimachine as compared to PMSG. For substations of tidal generations, the interconnection of multimachine requires the dynamic balance of system frequency and terminal voltage. Intensive investigations can be seen in the independent multimachine system. As a result, techniques, such as linear technology, fuzzy control, neural network, and sliding mode control, are often adopted in WRSG.

In this paper, the high-order sliding mode technology introduced in Levant (2005) is combined with multimachine system of tidal generators. The interconnection of multimachine in a finite system can be realized through the distributed control of a single generator. A 3-machine and 9-node system is simulated in MATLAB and the proposed control strategy is tested with mechanical perturbation.

SYSTEM AND METHODS

Hydraulic Turbine Model

The kinetic energy of seawater movement is given by:

$$P = \frac{1}{2}\rho S V^3 \tag{1}$$

For hydraulic turbine in the substation of tidal generations, only part of the kinetic energy mentioned in Equation (1) can be used. Given an arbitrary hydraulic turbine, *e.g.*, ith hydraulic turbine, the kinetic energy it can use is defined as:

$$P_{\mathrm{i}} = \frac{1}{2}\rho S_i V_{t_i}^3 \tag{2}$$

where ρ , S_{i} are the density of seawater and the cross-sectional area of the ith hydraulic turbine, respectively. is a constant for the use of kinetic energy, and is an empirical value in the range of 0.35~0.5 (Myers and Bahaj, 2006).

The velocity of the flow of seawater is as follows (Elghali, Benbouzid, and Charpentier, 2010):

$$V_{t_i} = V_{nt_i} + \frac{C_i - 45}{95 - 45}(V_{st_i} - V_{nt_i}) \tag{3}$$

DOI: 10.2112/SI103-076.1 received 18 September 2019; accepted in revision 15 March 2020.
*Corresponding author: mzhang@shmtu.edu.cn

where V_{st_i}, V_{nt_i} are the velocity of spring tide and neap tide at the ith node, respectively. The time interval between spring tide and neap tide is 6 hours. C_i is the tide constant at the ith node, which is normally in the range of 20~120.

To maximize the use of kinetic energy of seawater movement, the maximum power point tracking (MPPT) strategy is adopted to match the mechanical velocity of hydraulic turbine. This strategy generates the electromagnetic torque by the prediction of the velocity of seawater, behaving as a real hydraulic turbine in the simulation.

Multimachine System Model

Based on the multimachine models in power systems introduced in Damm, Marino, and Lamnabhi-Lagarrigue (2004), the model used in this paper is described as follows:

$$\begin{aligned} \dot{\delta}_i &= \omega_i \\ \dot{\omega}_i &= -\frac{D_i}{H_i}\omega_i - \frac{\omega_s}{H_i}(E'_{q_i} I_{q_i} - P_{m_i}) \\ \dot{E}'_{q_i} &= \frac{1}{T'_{d_i}}\left(E_{f_i} - E'_{q_i} - \left(X_{d_i} - X'_{d_i}\right) I_{d_i}\right) \end{aligned} \quad (4)$$

When $\omega_i = \omega_{g_i} - \omega_s$, $E_{f_i} = k_c u_{F_i}$, $P_{e_i} = E'_{q_i} I_{q_i}$, $0 < \delta < \pi$, $C_{q_i} = G_{ii}E'_{q_i} + \sum_{j=1\, j\neq i}^{n} E'_{q_j} \begin{Bmatrix} G_{ij}\cos(\delta_j - \delta_i) \\ -B_{ij}\sin(\delta_j - \delta_i) \end{Bmatrix}$

$I_{d_i} = -B_{ii}E'_{q_i} - \sum_{j=1\, j\neq i}^{n} E'_{q_j} \begin{Bmatrix} G_{ij}\sin(\delta_j - \delta_i) \\ +B_{ij}\cos(\delta_j - \delta_i) \end{Bmatrix}$, where $I_{d_i}(t)$, $I_{q_i}(t)$ $Vt_i = \sqrt{(E'_{q_i} - X'_{d_i} I_{d_i})^2 + (X'_{d_i} I_{q_i})^2}$ are the current in d-q coordinate system. $P_{e_i}(t)$ is the active electrical power of the ith generator. G_{ij} and B_{ij} are the conductance matrix and the admittance matrix of the system network, respectively. $E_{f_i}(t)$ is the equivalent electromotive force of the excitation coil. Vt_i is the terminal voltage. $\delta_i(t)$, $\omega_{g_i}(t)$, $E'_{q_j}(t)$, H_i, D_i, T'_{d0_i} denote power angle, electrical angular velocity, transient electromotive force, inertia coefficient, damping coefficient, and the time constant of the direct axis transient short circuit. ω_s is the rotating speed of the synchronous generator. X_{d_i}, X'_{d_i} are the direct axis reactance and the direct axis transient reactance, respectively.

The multimachine system modelled by Equation (4) can yield state equations as follows:

$$\begin{aligned} \dot{x}_{i_1} &= x_{i_2} \\ \dot{x}_{i_2} &= f_{i_1}(x) \\ \dot{x}_{i_3} &= f_{i_2}(x) + u_i \end{aligned} \quad (5)$$

$f_{i_1}(x) = a_i - b_i x_{i_2} - c_i x_{i_3}^2 - d_i x_{i_3} \sum_{j=1, j\neq i}^{n} x_{j_3} \begin{Bmatrix} G_{ij}\cos\left(x_{j_1} - x_{i_1}\right) \\ -B_{ij}\sin\left(x_{j_1} - x_{i_1}\right) \end{Bmatrix}$, $a_i = \frac{\omega_s}{H_i} P_{m_1}$,

$f_{i_2}(x) = -e_i x_{i_3} + h_i \sum_{j=1, j\neq i}^{n} x_{j_3} \begin{Bmatrix} G_{ij}\sin\left(x_{j_1} - x_{i_1}\right) \\ +B_{ij}\cos\left(x_{j_1} - x_{i_1}\right) \end{Bmatrix}$

$b_i = \frac{D_i}{H_i}$, $c_i = \frac{\omega_s}{H_i} G_{ii}$, $d_i = \frac{\omega_s}{H_i}$, $e_i = \frac{1 - \left(x_{d_i} - x'_{d_i}\right) B_{ii}}{T_{d_i}}$, $h_i = \frac{x_{d_1} - x'_{d_i}}{T_{d_i}}$,

$u_i = \frac{E_{f_1}}{T_{d_1}}$, $\mathbf{X}_i = \left[x_{i_1}, x_{i_2}, x_{i_3}\right]^T = \left[\delta_i(t), \omega_i(t), E'_{q_i}\right]^T$.

Controller Design

The control idea of traditional first order sliding mode has been developed by high order sliding mode, *i.e.*, the control variables are applied to the high order derivatives. The high order sliding mode remains the advances of traditional first order sliding mode, such as easy implementation, and strong robustness. Also, it can effectively eliminate system buffeting, minimize restrictions of relative order, and improve the control precision.

For each subsystem, a multimachine system can be considered a single input single output system with a degree of freedom r, which is defined as follows:

$$\sum_\sigma : \left\{\dot{x} = \tilde{f}(x) + \tilde{g}(x)\tilde{u},\ \tilde{\sigma} = \tilde{\sigma}(t,x)\right\} \quad (6)$$

where $x(t_0) = x_0, t_0 \geq 0$, $x \in B_x \subset \Re^k$ is a state vector, k is the dimension of the system in Equation (6), $\tilde{u} \subset \Re$ denotes the control input vector, $\tilde{f}$, $\tilde{g}$ are bounded smooth functions, $\tilde{\sigma} : \Re^{k+1} \to \Re$ (unknown), B_x is a finite subset centered at the origin.

In order for the system to converge in a finite time, the correlation r of the system is assumed to be a known constant, *i.e.*, the system can be controlled under the r-order derivative of $\tilde{\sigma}$:

$$\tilde{\sigma}^{(r)} = h(t,x) + m(t,x)\tilde{u} \quad (7)$$

When $h(t,x) = \sigma^{(r)}\big|_{\tilde{u}=0}$, $m(t,x) = \frac{\partial}{\partial u}\sigma^{(r)} \neq 0$, given K_m, K_M, $C > 0$, and satisfies:

$$0 < K_m \leq \frac{\partial}{\partial u}\sigma^{(r)} \leq K_M,\ \left|\sigma^{(r)}\big|_{\tilde{u}=0}\right| \leq C \quad (8)$$

i.e.:

$$\tilde{\sigma}^{(r)} \in \left[-C, C\right] + \left[K_m, K_M\right]\tilde{u} \quad (9)$$

As such, the bounded differential satisfies the Filippov property, *i.e.*, $\tilde{\sigma}^{(r)}$ can satisfy the condition of semi continuity, and thus, the control problem has solutions.

To design the high-order sliding mode control for the multimachine system in Equation (6), a k-dimension nonlinear sliding surface is given by:

$$\tilde{\sigma}\left(x, x^*\right) = 0 \quad (10)$$

where x^* is the equilibrium point of the system, $\sigma_i : \Re^k \to \Re$ and $\tilde{\sigma}(0) = 0$. Derivatives $\tilde{\sigma}, \tilde{\sigma}^{(1)}, \ldots, \tilde{\sigma}^{(r-1)}$ denote continuous functions of the state space vector of a closed system, and:

$$\tilde{\sigma} = \tilde{\sigma}^{(1} = \ldots = \tilde{\sigma}^{(r-1)} = 0 \quad (11)$$

Equation (11) is a non-null integral set, and is termed r-order sliding mode.

Based on the discuss above, controller is designed to stabilize the smooth system at the equilibrium point in a finite time, and is a quasi-continuous high order sliding mode controller (Equation (10) is not continuous).

The high-order sliding mode controller can be designed based on the equations below:

$$\begin{aligned}
&\phi_{0,r} = \tilde{\sigma}, N_{0,r} = \left|\tilde{\sigma}\right|, \\
&\Psi_{0,r} = \phi_{0,r} / N_{0,r} = sign\tilde{\sigma} \\
&\phi_{i,r} = \tilde{\sigma}^{(i)} + \tilde{\beta}_i N_{i-1,r}^{(r-i)/(r-i+1)} \Psi_{i-1,r} \\
&N_{i,r} = \left|\tilde{\sigma}^{(i)}\right| + \beta_i N_{i-1,r}^{(r-i)/(r-i+1)} \\
&\Psi_{i,r} = \phi_{i,r} / N_{i,r}
\end{aligned} \tag{12}$$

$\tilde{\beta}_1, ...\tilde{\beta}_{r-1}$, $\tilde{\alpha} > 0$, given the controller is:

$$\tilde{u} = -\tilde{\alpha}\Psi_{r-1,r} \tag{13}$$

The high order sliding mode controller for Equation (5) can be designed as follows:

$$\Sigma_{\sigma_i} : \begin{Bmatrix} \dot{\mathbf{X}}_i = \mathbf{F}_i(\mathbf{X}_i, \tilde{\mathbf{X}}_i) + \mathbf{M}u_i \\ \boldsymbol{\sigma}_i = \boldsymbol{\sigma}_i(\mathbf{X}_i, \mathbf{X}_i^{*}) \end{Bmatrix} \tag{14}$$

$\mathbf{X}_i^* = (x_{i_1}^*, x_{i_2}^*, x_{i_3}^*)$, $\mathbf{X}^* = \left[X_1^*, ..., X_n^*\right]$, $\tilde{\mathbf{X}} = \left[X_1, ..., X_{i-1}, X_{i+1}, ..., X_n\right]^T$ is the equilibrium point of the multimachine system based on Equation (5).

$\mathbf{F}_i = \begin{bmatrix} x_{i_2} \\ f_{i_1}(\mathbf{X}_i, \tilde{\mathbf{X}}_i) \\ f_{i_2}(\mathbf{X}_i, \tilde{\mathbf{X}}_i) \end{bmatrix}$, $\mathbf{M} = \begin{bmatrix} 0 \\ 0 \\ 1 \end{bmatrix}$. The sliding mode surface of each subsystem Σ_{σ_i} is defined as:

$$\begin{aligned}
&\sigma_i = x_{i_1} - x_{i_1}^* \\
&\dot{\sigma}_i(\mathbf{X}_i, \mathbf{X}_i^*) = x_{i_2} \\
&\ddot{\sigma}_i(\mathbf{X}_i, \mathbf{X}_i^*) = a_i - b_i x_{i_2} - c_i x_{i_3}^2 - d_i x_{i_3} I_{q_i} \\
&i = 1, ..., n
\end{aligned} \tag{15}$$

The control rule of the sliding mode is:

$$\begin{aligned}
&u_i = -\alpha_i \frac{A_i}{B_i} \\
&A_i = \ddot{\sigma}_i + 2(\left|\dot{\sigma}_i\right| + \left|\sigma_i\right|^{\frac{2}{3}})^{\frac{-1}{2}} * (\dot{\sigma}_i + \left|\sigma_i\right|^{\frac{2}{3}} sign\sigma_i) \\
&B_i = \left|\ddot{\sigma}\right| + 2(\left|\dot{\sigma}_i\right| + \left|\sigma^{\frac{2}{3}}\right|)^{\frac{1}{2}}
\end{aligned} \tag{16}$$

Simulation Results

The multimachine model of tidal generator is shown in Figure 1. The connection network of multimachine system is delineated in Figure 2. The independent power network is composed of a three-machine system. The related parameters of the generator are listed in Table 1. The equilibrium point of each generator is known. The mechanical faults of the blades of tidal generators are often caused by alga and fishing nets. Simulations in MATLAB are applied to evaluate the robustness of the system.

Parameters for the equilibrium points of generators:

$$\begin{cases} x_{11}^* = 0.0395, x_{12}^* = 0, x_{13}^* = 1.0565 \\ x_{21}^* = 0.3443, x_{22}^* = 0, x_{23}^* = 1.0503 \\ x_{31}^* = 0.2301, x_{32}^* = 0, x_{33}^* = 1.0171 \end{cases}.$$

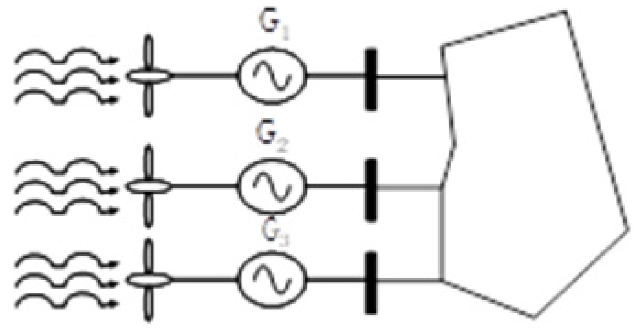

Figure 1. Tidal generators Multimachine mode.

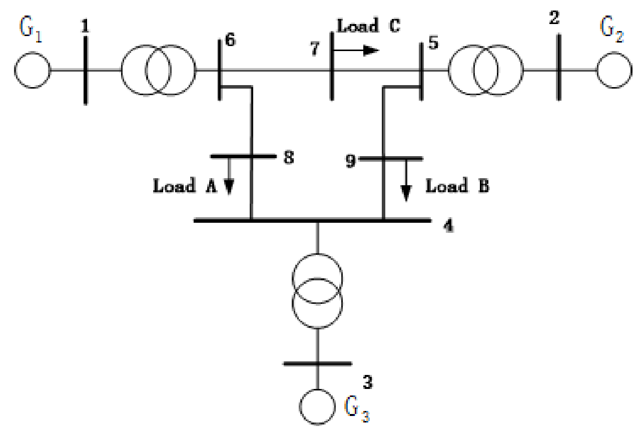

Figure 2. Multimachine system connection.

Table 1. *Generator parameters.*

Parameter	G1	G2	G3
H(seg)	23.64	6.4	3.01
x_d(pu)	0.146	0.8958	1.3125
x'_d(pu)	0.0608	0.1198	0.1813
D(pu)	0.3100	0.5350	0.6000
P_m(pu)	0.7157	1.6295	0.8502
T'_{d0}(pu)	8.96	6.0	5.89

Parameters for the multimachine network:

$$G = \left[G_{ij}\right] = \begin{bmatrix} 0.8453 & 0.2870 & 0.2095 \\ 0.2870 & 0.4199 & 0.2132 \\ 0.2095 & 0.2132 & 0.2770 \end{bmatrix},$$

$$B = \left[B_{ij}\right] = \begin{bmatrix} -2.9882 & 1.5130 & 1.2256 \\ 1.5130 & -2.7238 & 1.0879 \\ 1.2256 & 1.0879 & -2.3681 \end{bmatrix}.$$

In this paper, the following experiments are performed to test the robustness of the proposed control strategy.

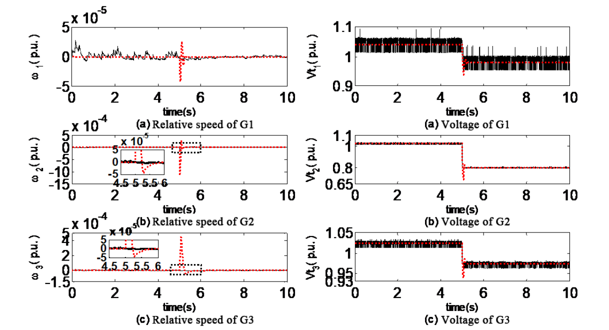

Figure 3. Relative speed and Terminal voltage of G1, G2, G3.

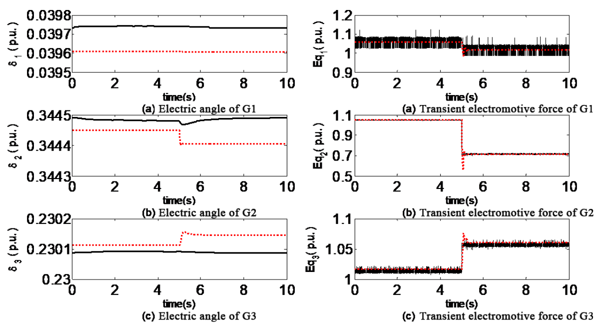

Figure 4. Power angle and Transient EMF in the quadrature axis of G1, G2, G3.

The hydraulic turbine connected to G2 has a permanent fault:

1. When t=0 s, the system is in a condition before failure.
2. When t=5 s, the output power of hydraulic turbine decreases by 30%, the system is running in this condition.

Figure 3 and Figure 4 illustrate the comparison between the control strategy proposed in this paper and traditional low-order sliding mode control. In both figures, the dash line denotes the control strategy proposed by the authors, and the solid line denotes traditional sliding mode control. It can be seen that high order sliding mode control can be more advantageous than traditional low order sliding mode control in the suppression of buffeting. When system is in a steady status, the proposed control strategy can present better results than traditional low order sliding mode control, while robustness of low order sliding mode control is slightly better than the proposed control strategy when system is in a fault condition.

The advance of proposed control strategy also embodies in the control of frequency and terminal voltage of the multimachine system, and thus, the system can be remained in a dynamic balance. In the meantime, the system can be stabilized within a short time when a fault occurs through the control of controller.

CONCLUSIONS

In this paper, a nonlinear discrete sliding mode control strategy has been proposed in the combination of the concept of high-order sliding mode control. The results demonstrate that the system can converge to its equilibrium point in a finite time when the strategy is applied to the excitation of synchronous generators in multimachine systems.

In combination of the MPPT control of hydroturbines, the control strategy applied to multimachine systems in an independent tidal generation can effectively increase the kinetic energy extracted from seawater movement and realize the frequency stability and voltage balance of multimachine systems in the substations of tidal generations.

Also, simulations of multimachine systems in MATLAB demonstrate that the effectiveness and robustness of the proposed control strategy in the improvement of the system stability when the system experiences mechanical perturbations.

LITERATURE CITED

Bai, Y.; Du, M.; Zhou, Q.; Meng, J., and Wu, H., 2016. Proceeding of tidal current energy conversion system. *Ocean Development and Management*, (3), 57-63.

Boye, H.; Caquot, E., and Clement, P., 2013. Rapport de la mission d'étude sur les énergies marines renouvelables.

Damm, G.; Marino, R., and Lamnabhi-Lagarrigue, F., 2004. Adaptive nonlinear output feedback for transient stabilization and voltage regulation of power generators with unknown parameters. *International Journal of Robust & Nonlinear Control*, 14(9-10), 833–855.

Elghali, S.E.B.; Benbouzid, M.E.H., and Charpentier, J.F., 2010. Modélisation et commande d'une hydrolienne équipée d'une génératrice asynchrone double alimentation. *European Journal of Electrical Engineering*, 13(2), 161-178.

Gu, Y.; Yin, X., and Liu, H., 2015. Fuzzy terminal sliding mode control for extracting maximum marine current energy. *Energy*, 90, 258-265.

Jiang, J.; Sun, K.; Zheng, X., and Ju, Q., 2019. The blade pitching optimization method of vertical axis tidal turbine to maximum power coefficient. *EKOLOJI*, 28, 1173-1184.

Levant, A., 2005. Homogeneity approach to high-order sliding mode design. *Automatica*, 41(5), 823-830.

Ma, Y.; Lam, W.H.; Cui, Y.; Zhang, T.; Jiang, J.; Sun, C.; Guo, J.; Wang, S.; Lam, S.S., and Hamill, G., 2018. Theoretical vertical-axis tidal-current-turbine wake model using axial momentum theory with CFD corrections. *Applied Ocean Research*, 79, 113-122.

Ma, Y.; Li, T.; Zhang, X., and Zhang, L., 2015. Research on coupling prediction of mooring line tension and motion response of vertical axis floating tidal energy converter. *In:* Makowski, C. (ed.), *Recent Developments of Port and Ocean Engineering*. *Journal of Coastal Research*, Special Issue No. 1, pp. 496-504.

Myers, L. and Bahaj, A.S., 2006. Power output performance characteristics of a horizontal axis marine current turbine. *Renewable Energy*, 31(2), 197-208.

Psillakis, H.E. and Alexandridis, A.T., 2005. A new excitation control for multi-machine power systems 1: Decentralized nonlinear adaptive control design and stability analysis. *International Journal of Control Automation & Systems*, 3(2), 288-295.

Sun, C.; Lam, W.H.; Cui, Y.; Zhang, T.; Jiang, J.; Guo, J.; Ma, Y.; Wang, S.; Tan, T.H.; Chuah, J.H.; Lam, S.S., and Hamill, G., 2018. Empirical model for Darrieus-type tidal current turbine induced seabed scour. *Energy Conversion Management*, 171, 478-490.

Xu, X.; Zhao, H.; Zhen, Z.; Wang, C., and Shi, W., 2015. Numerical research on dynamic water-head of gulf tidal energy: A new exploration on development way of tidal energy. *In:* Makowski, C. (ed.), *Recent Developments of Port and Ocean Engineering*. *Journal of Coastal Research*, Special Issue No. 1, pp. 331-336.